Bulk properties of composite media. II. Evaluation of bounds on the shear modulus of suspensions of impenetrable spheres

Asok K. Sen
Department of Mechanical and Aerospace Engineering, North Carolina State University, Raleigh, North Carolina 27695-7910

F. Lado
Department of Physics, North Carolina State University, Raleigh, North Carolina 27695-8202

S. Torquato
Department of Mechanical and Aerospace Engineering and Department of Chemical Engineering, North Carolina State University, Raleigh, North Carolina 27695-7910

(Received 22 June 1987; accepted for publication 5 August 1987)

We evaluate third-order bounds due to Milton and Phan-Thien on the effective shear modulus G_e of a random dispersion of identical impenetrable spheres in a matrix up to sphere-volume fractions near the random close-packing value. The third-order bounds, which incorporate two parameters, ζ_2 and η_2, that depend upon the three-point probability function of the composite medium, are shown to significantly improve upon the second-order Hashin–Shtrikman (or, more general, Walpole) bounds which do not utilize this information, for a wide range of volume fraction and phase property values. The physical significance of the microstructural parameter η_2 for general microstructures is briefly discussed. The third-order bounds on G_e are found to be sharp enough to yield good estimates of the effective shear modulus for a wide range of sphere-volume fractions, even when the individual shear moduli differ by as much as two orders of magnitude. Moreover, when the spheres are highly rigid relative to the matrix, the third-order lower bound on the effective property provides a useful estimate of it. The third-order bounds are compared with experimental data for the shear modulus of composites composed of glass spheres in an epoxy matrix and the shear viscosity of suspensions of bituminous particles in water. In general, the third-order lower bound (rather than the upper bound) on G_e tends to provide a good estimate of the data.

I. INTRODUCTION

In a previous article[1] (henceforth referred to as I) on the study of third-order bounds on the effective shear modulus of two-phase disordered composite media, we simplified one of the key multidimensional cluster integrals η_2 that arises for the model of a distribution of identical, impenetrable spheres in a matrix. The other cluster integral ζ_2 which is required here (as well as in the third-order bounds on the effective conductivity and the bulk modulus), has already been simplified and tabulated by Torquato and Lado[2] for a random suspension of spheres. In this article we compute the microstructural parameter η_2 for the same model. The third-order McCoy[3] and the Milton–Phan-Thien[4] (MPT) bounds on the effective shear modulus G_e, which depend upon ζ_2 and η_2, are then evaluated for the aforementioned model.

The phase volume fractions, bulk moduli, and shear moduli are denoted, respectively, by ϕ_1 and ϕ_2, K_1 and K_2, and G_1 and G_2, where phase 1 is the matrix phase and phase 2 is the included phase. In Sec. II, we present the MPT bounds on G_e and the simplified expression for η_2 as obtained from I. In Sec. III, we calculate η_2 for our model up to a sphere-volume fraction $\phi_2 = 0.60$. This important microstructural parameter η_2, which depends upon a certain three-point probability function of the composite, is calculated here and compared to the corresponding values for two other models. Such comparisons for ζ_2 were already made by Torquato and Lado.[2] Using the results of Sec. III, the third-order bounds on G_e for a random dispersion of impenetrable spheres are computed up to densities near the random close-packing value. In each of the cases considered, we compare the third-order MPT bounds with the second-order (and, hence less restrictive) Hashin–Shtrikman[5] (HS) or Walpole[6] bounds. The former second-order bounds are actually special cases of the latter. Here we also compare the third-order bounds on G_e with experimental data for the shear modulus obtained by Smith[7] for glass-epoxy composites, and with data on shear viscosity of suspensions of bituminous particles in water obtained by Eilers.[8] Finally, in Sec. V, we make some concluding remarks.

II. THIRD-ORDER BOUNDS ON THE SHEAR MODULUS FOR SUSPENSIONS OF IMPENETRABLE SPHERES

The third-order McCoy bounds[3] on the shear modulus, as simplified by Milton,[9] depend not only upon the individual phase properties K_1, K_2, G_1, G_2, and volume fraction ϕ_2, but also on two different integrals (defined below) involving the three-point probability function $S_3(r,s,t)$ of the medium, a quantity that gives the probability of finding the vertices of a triangle of sides r, s, and t, in one of the phases, say phase 2 (as is the convention in this work).[10] Milton and Phan-Thien[4] (MPT) obtained new improved third-order bounds that depend on the same set of parameters as the simplified McCoy bounds. For conciseness, we present here only the MPT bounds, which read

 0021-8979/87/224135-07$02.40

$$\left(\langle G\rangle - \frac{6\phi_1\phi_2(G_1-G_2)^2}{6\langle\tilde{G}\rangle + \Xi^{-1}}\right) < G_e < \left(\langle G\rangle - \frac{6\phi_1\phi_2(G_1-G_2)^2}{6\langle\tilde{G}\rangle + \theta}\right), \tag{1}$$

where

$$\Xi = \frac{5\left\langle\frac{1}{G}\right\rangle_\zeta\left\langle\frac{6}{K}-\frac{1}{G}\right\rangle_\zeta + \left\langle\frac{1}{G}\right\rangle_\eta\left\langle\frac{2}{K}+\frac{21}{G}\right\rangle_\zeta}{\left\langle\frac{128}{K}+\frac{99}{G}\right\rangle_\zeta + 45\left\langle\frac{1}{G}\right\rangle_\eta}, \tag{2}$$

$$\theta = \frac{3\langle G\rangle_\eta\langle 6K+7G\rangle_\zeta - 5\langle G\rangle_\zeta^2}{\langle 2K-G\rangle_\zeta + 5\langle G\rangle_\eta}, \tag{3}$$

and where the angular brackets denote the averages of the following types for any property b,

$$\begin{aligned}\langle b\rangle &= b_1\phi_1 + b_2\phi_2,\\ \langle b\rangle_\zeta &= b_1\zeta_1 + b_2\zeta_2,\\ \langle b\rangle_\eta &= b_1\eta_1 + b_2\eta_2,\\ \langle\tilde{b}\rangle &= b_1\phi_2 + b_2\phi_1.\end{aligned} \tag{4}$$

Here the quantities ζ_i and η_i $(i=1,2)$ are integrals which depend upon the three-point probability function S_3:

$$\zeta_2 = 1-\zeta_1 = (9/2\phi_1\phi_2)I(\hat{S}_3), \tag{5}$$

$$\eta_2 = 1-\eta_1 = \tfrac{5}{21}\zeta_2 + (150/7\phi_1\phi_2)J(\hat{S}_3), \tag{6}$$

and

$$\hat{S}_3(r_{12},r_{13},r_{23}) = S_3(r_{12},r_{13},r_{23}) - [S_2(r_{12})S_2(r_{13})]/\phi_2, \tag{7}$$

and where the integral operators I and J for some function $f(r_{12},r_{13},r_{23})$ are defined as

$$I[f] = \frac{1}{8\pi^2}\int d\mathbf{r}_2\,d\mathbf{r}_3 f(r_{12},r_{13},r_{23})\frac{P_2(\hat{\mathbf{r}}_{12}\cdot\hat{\mathbf{r}}_{13})}{r_{12}^3 r_{13}^3}, \tag{8}$$

and

$$J[f] = \frac{1}{8\pi^2}\int d\mathbf{r}_2\,d\mathbf{r}_3 f(r_{12},r_{13},r_{23})\frac{P_4(\hat{\mathbf{r}}_{12}\cdot\hat{\mathbf{r}}_{13})}{r_{12}^3 r_{13}^3}. \tag{9}$$

Here S_2 is the two-point probability function in the particulate phase, $r_{ij} = |\mathbf{r}_i - \mathbf{r}_j|$, $\hat{\mathbf{r}}_{ij} = \mathbf{r}_{ij}/r_{ij}$, and P_l, the Legendre polynomial of degree l. The form of Eq. (7) ensures the absolute convergence of these integrals.

One can easily show that for $\zeta_2 = \eta_2 = 0$ (or $\zeta_1 = \eta_1 = 1$), the third-order bounds (1) coincide and collapse onto the second-order HS lower bound for $(K_1-K_2)(G_1-G_2) > 0$. Similarly, it may be shown that for $\zeta_2 = \eta_2 = 1$ (or $\zeta_1 = \eta_1 = 0$), the MPT upper and lower bounds coincide and merge with the HS upper bound for $(K_1-K_2)(G_1-G_2) > 0$. The fact that both ζ_2 and η_2 (for any geometry) must always lie between 0 and 1 implies that the third-order bounds always improve upon the second-order Walpole bounds or, where appropriate, HS bounds.

In order to compute the bounds on shear modulus as described above, one must calculate $I[\hat{S}_3]$ and $J[\hat{S}_3]$ for the microstructure of interest. For the model of random impenetrable-spherical inclusions in a matrix, Torquato and Lado[2] evaluated $I[\hat{S}_3]$. In I we simplified the cluster integral $J[\hat{S}_3]$ for this model and found for spheres of radius a that

$$J[\hat{S}_3] = \frac{1}{8\pi^2}\phi_2^2\int d\mathbf{r}\,g(r)W_2(r) + \frac{\phi_2^3}{16\pi^2}\int d\mathbf{r}_2\,d\mathbf{r}_3[g_3(r_{12},r_{13},r_{23}) - g(r_{12})g(r_{13})]Q(r_{12},r_{13},r_{23}), \tag{10}$$

where

$$W_2(r) = \frac{4}{3}\pi\left(\frac{a^3}{(r^2-a^2)^3} - \frac{14}{5}\frac{a^5}{(r^2-a^2)^4} - \frac{63}{25}\frac{a^7}{(r^2-a^2)^5} + \frac{196}{25}\frac{a^9}{(r^2-a^2)^6} + \frac{168}{25}\frac{a^{11}}{(r^2-a^2)^7}\right), \tag{11}$$

and

$$Q(r_{12},r_{13},r_{23}) = \frac{14}{5!}\sum_{l=4}^{\infty} l(l-1)(l-2)(l-3)\frac{(2l-3)}{(2l-1)}\frac{a^{2l-8}}{r_{12}^{l-1}r_{13}^{l-1}} \times\left[1-\frac{2}{5}(l+1)\left(\frac{2l-1}{2l-3}\right)\left(\frac{a}{r_{12}}\right)^2\right]\left[1-\frac{2}{5}(l+1)\left(\frac{2l-1}{2l-3}\right)\left(\frac{a}{r_{13}}\right)^2\right]P_l(\cos\theta_{213}) + \frac{8}{5!}\sum_{l=3}^{\infty}\frac{l(l-1)(l-2)(11l+15)}{(2l+3)(2l-3)}\frac{a^{2l-4}}{r_{12}^{l+1}r_{13}^{l+1}}P_l(\cos\theta_{213}). \tag{12}$$

Here $g(r)$ is the pair distribution function, $g_3(r_{12},r_{13},r_{23})$ is the three-particle distribution function, and $\cos\theta_{213} = \hat{\mathbf{r}}_{12}\cdot\hat{\mathbf{r}}_{13}$. Thus, for impenetrable spherical suspensions, we may write

$$J[\hat{S}_3] = k_2\phi_2^2 + k_3\phi_3^3, \tag{13}$$

where

$$k_2 = \frac{1}{8\pi^2}\int d\mathbf{r}\,g(r)W_2(r) \tag{14}$$

and

$$k_3 = \frac{1}{16\pi^2}\int d\mathbf{r}_2\,d\mathbf{r}_3[g_3(r_{12},r_{13},r_{23}) - g(r_{12})g(r_{13})] \times Q(r_{12},r_{13},r_{23}). \tag{15}$$

III. THREE-POINT PARAMETER η_2 FOR IMPENETRABLE SPHERES

A. Calculation of η_2

The three-point microstructural parameter η_2, just like the other three-point parameter ζ_2, for a suspension of identical impenetrable spheres, depends upon the pair and triplet distribution functions[11] of hard spheres, as given by Eq. (10). Here we assume an equilibrium distribution of rigid spheres. The pair distribution function for this model is available from the accurate fit of Verlet and Weis.[12] However, this parametrization does not seem to be very reliable close to the random close-packing volume fraction value of about 0.64[13]; thus the highest ϕ_2 reported in this paper is 0.60, for which the Verlet–Weis results still show their expected internal consistency. The triplet distribution function is more problematical. Lacking any more fundamental alternative, we employ the Kirkwood superposition approximation,

$$g_3(r_{12},r_{13},r_{23}) \approx g(r_{12})g(r_{13})g(r_{23}) , \tag{16}$$

in our calculations.

To facilitate numerical work, we replace $g(r)$ in the expression for k_2, Eq. (14), by $1+h(r)$. Also, we choose a length scale in which the radius of a hard sphere is unity. Then one can obtain

$$k_2 = \frac{7213}{109\,350} - \frac{1}{24}\ln 3 + \frac{1}{2\pi}\int_2^\infty dr\, r^2 h(r) W_2(r) , \tag{17}$$

where $W_2(r)$ is now given by (11) with $a=1$. This form has the advantage that the integrand in (17) vanishes rapidly for large r. In the superposition approximation, k_3 of Eq. (15) becomes

$$k_3 = \frac{14}{5!}\sum_{l=4}^{\infty}\frac{l(l-1)(l-2)(l-3)(2l-3)}{(2l-1)(2l+1)}\int_2^\infty dr_{12}\frac{g(r_{12})}{r_{12}^{l-3}}\left[1-\frac{2(l+1)(2l-1)}{5(2l-3)}\left(\frac{1}{r_{12}}\right)^2\right]$$
$$\times\int_2^\infty dr_{13}\frac{g(r_{13})}{r_{13}^{l-3}}\left[1-\frac{2(l+1)(2l-1)}{5(2l-3)}\left(\frac{1}{r_{13}}\right)^2\right]H_l(r_{12},r_{13})$$
$$+\frac{8}{5!}\sum_{l=3}^{\infty}\frac{l(l-1)(l-2)(11l+15)}{(2l-3)(2l+1)(2l+3)}\int_2^\infty dr_{12}\frac{g(r_{12})}{r_{12}^{l-1}}\int_2^\infty dr_{13}\frac{g(r_{13})}{r_{13}^{l-1}}H_l(r_{12},r_{13}) , \tag{18}$$

where

$$H_l(r_{12},r_{13}) = \frac{2l+1}{2}\int_{-1}^{1} d(\cos\theta_{213})h(r_{23})P_l(\cos\theta_{213}) \tag{19}$$

and $r_{23}^2 = r_{12}^2 + r_{13}^2 - 2r_{12}r_{13}\cos\theta_{213}$. Using the Fourier transform $\tilde{h}(k)$ of $h(r)$, we can write the coefficient H_l as (see Appendix A of I)

$$H_l(r_{12},r_{13}) = \frac{2l+1}{2\pi^2}\int_0^\infty dk\, k^2\tilde{h}(k)j_l(kr_{12})j_l(kr_{13}) , \tag{20}$$

where j_l is the spherical Bessel function of order l. Using this result, we can simplify (18) as

$$k_3 = \frac{1}{2\pi^2}\int_0^\infty dk\, k^2\tilde{h}(k)\sum_{l=4}^{\infty}(l-1)(l-2)(l-3)$$
$$\times\left[\frac{7l(2l-3)}{60(2l-1)}\left(A_l(k)-\frac{2(l+1)(2l-1)}{5(2l-3)}B_l(k)\right)^2 + \frac{11l+4}{15(2l-5)(2l+1)}[B_{l-1}(k)]^2\right] , \tag{21}$$

where

$$A_l(k) = \int_2^\infty dr\, g(r)\frac{j_l(kr)}{r^{l-3}} = \frac{j_{l-1}(2k)}{2^{l-3}k} + \frac{j_{l-2}(2k)}{2^{l-3}k^2} + \int_2^\infty dr\, h(r)\frac{j_l(kr)}{r^{l-3}} \tag{22}$$

and

$$B_l(k) = \int_2^\infty dr\, g(r)\frac{j_l(kr)}{r^{l-1}} = \frac{j_{l-1}(2k)}{2^{l-1}k} + \int_2^\infty dr\, h(r)\frac{j_l(kr)}{r^{l-1}} . \tag{23}$$

The integrals in (21)–(23) were done numerically using upper cutoff lengths of r_{max} and k_{max}, respectively, in real and Fourier space. r_{max} was chosen such that $g(r)$, as obtained from the above-mentioned Verlet–Weis fit, does not differ from 1 (for r close to r_{max}) by more than the accuracy requirement we imposed. Then k_{max} was automatically determined by our choice of Δr ($k_{max} = \pi/\Delta r$), selected to make real-space integrals stable up to the desired number of significant figures (usually up to 4). This also fixed the mesh size for the Fourier space integration: $\Delta k = \pi/r_{max}$. Finally, a choice for l_{max}, the maximum value for the number of terms in the sum over l (which, in principle, goes up to ∞), is needed. This number was found to be about 10 for low volume fractions and about 12 for high volume fractions for a precision requirement of 10^{-5}. The numerical procedure described here was the same one employed by Torquato and Lado[2] to compute ζ_2.

B. Results and discussion

In Table I the three-point parameters ζ_2 and η_2 are presented for randomly and isotropically distributed identical, impenetrable spheres in a matrix phase for selected volume fractions in the range $0 \leqslant \phi_2 \leqslant 0.6$. The values of ζ_2 are actually taken from Ref. 2. A study by Beasley and Torquato[14] indicates that the use of the superposition approximation to compute ζ_2 underestimates the exact ζ_2; however, the errors

TABLE I. Three-point parameters ζ_2 (Ref. 2) and η_2 for an equilibrium distribution of equal-sized impenetrable spheres in a matrix.

ϕ_2	ζ_2	η_2
0.0	0.0	0.0
0.05	0.0104	0.0244
0.10	0.0205	0.0493
0.15	0.0303	0.0746
0.20	0.0398	0.100
0.25	0.0492	0.127
0.30	0.0588	0.154
0.35	0.0695	0.183
0.40	0.0836	0.216
0.45	0.105	0.255
0.50	0.141	0.306
0.55	0.205	0.378
0.60	0.328	0.491

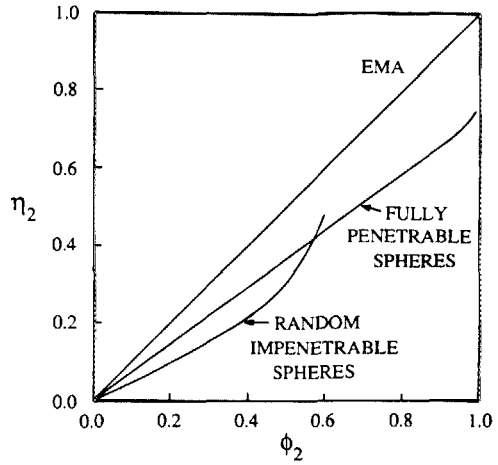

FIG. 1. Three-point parameter η_2 for the class of models corresponding to the EMA, for random distribution of equal-sized fully penetrable spheres (Ref. 17) and for the equal-sized random impenetrable-sphere model calculated here.

introduced in using the superposition approximation (which increase as the close-packing volume fraction is approached) were shown not to be serious. Since the integrals associated with ζ_2 are of the same form as the corresponding integrals of η_2, it is expected that application of the superposition approximation (16) in Eq. (15) should not lead to large errors in η_2.

The physical significance of the microstructural parameters ζ_2 and η_2 have not yet been fully elucidated for arbitrary composite media. Torquato and Lado[2] have recently discussed the significance of ζ_2 for a number of different microstructures. In Fig. 1 the three-point parameter η_2 is plotted as a function of ϕ_2 for three different models: a certain class of granular materials[15] corresponding to the effective-medium approximation[16] (EMA) for which $\eta_2 = \phi_2$, fully penetrable (randomly centered) spheres,[17] and the equilibrium distribution of impenetrable spheres studied here. Qualitatively, the comments made in Ref. 2 regarding ζ_2 for the geometries of Fig. 1 apply as well to η_2. For example, for the three models, η_2 is a monotomically increasing function of ϕ_2. We find again that the absence of spatial correlation in the case of fully penetrable spheres leads to a parameter η_2 which is approximately linear over the entire range of ϕ_2. For the EMA geometry and the related[15] symmetric-cell material[18] (with spherical cells) η_2 is exactly linear in ϕ_2, namely, $\eta_2 = \phi_2$. Comparisons between these latter two microstructures and fully penetrable spheres were described in Ref. 2. We note that exclusion-volume effects present in the impenetrable-sphere case are responsible for both ζ_2 and η_2 lying below the corresponding values for fully penetrable spheres at low volume fractions and for the precipitous increase of these parameters as the close-packing volume fraction is approached. As a final point here, we note that it is the property of polydispersity in the grain sizes, along with the absence of correlation between two types of grains, which makes η_2 for the models corresponding to the EMA even larger.

Note that η_2 for the impenetrable spheres crosses the η_2 for penetrable spheres at $\phi_2 \cong 0.57$. Although this crossing effect was not explicitly observed for the case of ζ_2 in three dimensions, the trend is nonetheless present there (see Ref. 2). Such an effect has also been observed[19] for ζ_2 for circular inclusions in 2D (or oriented infinitely long cylinders in 3D). Thus, there does not seem to be any inconsistency involved here, although it may be against intuition at first sight. The physical significance of this effect has been given elsewhere.[19]

IV. EVALUATION OF BOUNDS ON THE SHEAR MODULUS OF A SUSPENSION OF IMPENETRABLE SPHERES

Using the results of the previous section (Table I for ζ_2 and η_2), we evaluate the third-order MPT bounds on the shear modulus for a random distribution of equal-sized impenetrable spheres in a matrix for $0 \leqslant \phi_2 \leqslant 0.6$. For the presentation of our results, it is useful to define the following parameters: $\alpha = K_2/K_1, \beta = G_2/G_1, \gamma_1 = G_1/K_1, \gamma_2 = G_2/K_2$. Since $\alpha\gamma_2 = \beta\gamma_1$, only three of these are independent. Also, since $\gamma = (3 - 6\nu)/(2\nu + 2)$, where ν is the Poisson's ratio and since $0 \leqslant \nu \leqslant 0.5$, we must have $0 \leqslant \gamma_i \leqslant 1.5$ $(i = 1,2)$. It may be mentioned here that we also calculated the third-order (but less restrictive) McCoy bounds for all the corresponding cases, but the differences between the McCoy and MPT bounds were imperceptible (even though the differences increase at higher ϕ_2) on the scales of our figures, except when $\beta \gg 1$. For example, for $\beta = 10^5$, $\gamma_1 = 0$, $\gamma_2 = 0.6$; the McCoy lower bound for G_e/G_1 is 6.92 and that for the MPT lower bound is 7.04 at a volume fraction $\phi_2 = 0.6$. The upper bounds for this case are identical up to four digits for all volume fractions. Hence, we have presented only the MPT bounds in all our figures. In all the cases presented here, we have compared the third-order bounds with the second-order HS bounds, which in fact are special cases of the more general Walpole bounds. In two cases, the bounds have been compared with available experimental data. The first is that of Smith[7] for the effective shear modulus of glass spheres embedded in an epoxy matrix where the ratio of the shear moduli is moderately high. The second is that of Eilers[8] for the effective shear viscosity of bituminous particles in water which represents a limiting case where the ratio

of the shear viscosities is very large and the fluid (matrix) is incompressible.

Before proceeding any further, we would like to make some general comments. For any given volume fraction ϕ_2, and for fixed γ_1 and γ_2, all the nth order lower bounds (with a finite n) tend to zero as either α or $\beta \to 0$ and all the nth order upper bounds tend to infinity as either α or $\beta \to \infty$. However, these facts do not reduce the importance of the bounds because of the following reasons. First of all, as previously mentioned, the bounds become progressively tighter as one goes to higher order. More importantly, Torquato[20] has observed that depending upon whether the composite is above or below its percolation threshold, one of the bounds will give the estimate of the property, even though the other bound diverges from it. For example, the lower-order *lower* bounds (such as second-, third-, and fourth-order lower bounds) should yield good estimates of G_e for $\beta \gg 1$, provided that ϕ_2 is below the percolation-threshold value ϕ_2^c and $\Lambda_2 \ll L$, where Λ_2 is the mean cluster size[21] of phase 2 and L is the scaled characteristic length[22] of the sample. Clearly, if the latter condition is satisfied, so is the former. Similarly, lower-order *upper* bounds should yield good estimates of the effective property for $\beta \gg 1$, provided that $\phi_2 > \phi_2^c$ and $\Lambda_1 \ll L$, where Λ_1 is the mean cluster size of phase 1. For our equilibrium model, the coordination number (i.e., the average number of spheres physically touching each sphere) is zero for all ϕ_2 except at the random close-packing value. In other words, the condition $\Lambda_2 \ll L$ is satisfied for all ϕ_2 except at the percolation point. Hence, the third-order lower bound should serve as a good estimate of G_e for all $\beta > 1$ and for all ϕ_2 provided that the system is not in the near critical regime (cf. subsequent discussion of Fig. 7).

Figures 2 and 3 compare the second-order HS bounds on G_e/G_1 to the MPT upper and lower bounds (1) for an equilibrium distribution of impenetrable spheres in a matrix

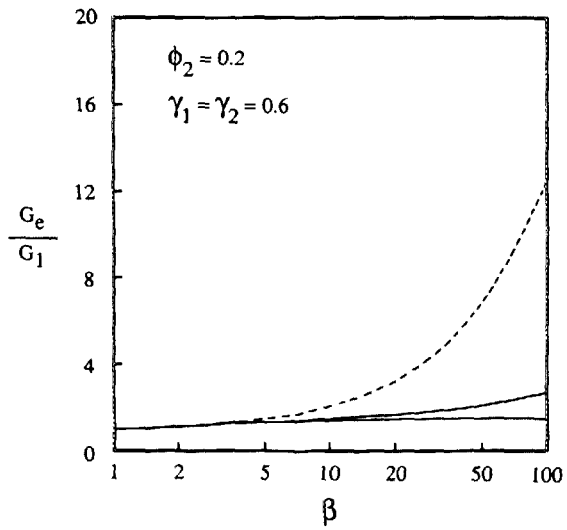

FIG. 2. Upper and lower bounds on the reduced effective shear modulus G_e/G_1 for the range $1 \leqslant \beta \leqslant 100$ at $\phi_2 = 0.2$. Second-order HS (Ref. 5) bounds (dashed lines); third-order MPT (Ref. 4) bounds for the equal-sized random impenetrable-sphere model (solid lines). Here $\beta = G_2/G_1$, $\alpha = K_2/K_1 = \beta$, $\gamma_1 = G_1/K_1 = 0.6$, and $\gamma_2 = G_2/K_2 = 0.6$. On the scale of this figure, the third-order lower bound is indistinguishable from the second-order lower bound.

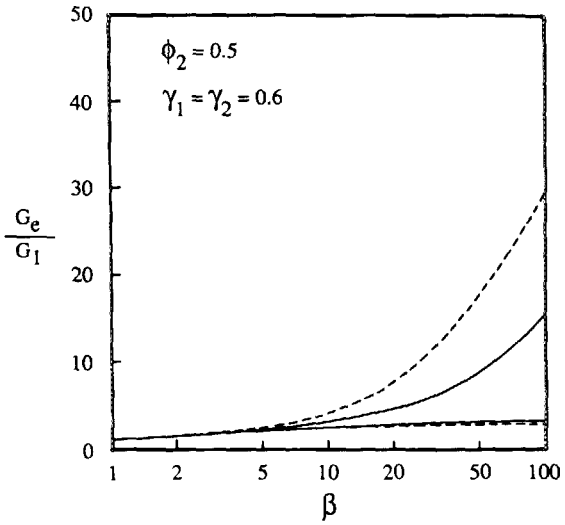

FIG. 3. As for Fig. 2 with $\phi_2 = 0.5$.

for $1 \leqslant \beta \leqslant 100$ ($\alpha = \beta$) at $\phi_2 = 0.2$ and $\phi_2 = 0.5$, respectively. One can clearly see that for low to moderate concentrations, the improvement in the width of the bounds in going from second- to third-order is tremendous even when the particles are two orders of magnitude more rigid than the matrix and that most of this improvement has occurred in the upper bound rather than the lower bounds for reasons mentioned above. For $\beta = 10$ and $\phi_2 = 0.2$, Fig. 2 shows that the third-order bounds are about ten times narrower than the second-order bounds. At the same volume fraction for $\beta = 100$, the third-order bounds are about 9.1 times more restrictive than the second-order bounds. For $\phi_2 = 0.5$, Fig. 3 shows that the third-order bounds are 3.3 and 2.5 times narrower than the second-order bounds for $\beta = 10$ and 100, respectively. Thus, for $1 \leqslant \beta \leqslant 100$, the MPT bounds are sufficiently restrictive so as to provide useful estimates of the effective shear modulus for a wide range of ϕ_2. Corresponding curves for $0.01 \leqslant \beta \leqslant 1$ are not presented because they are qualitatively similar to Figs. 2 and 3, except in this case the improvement is in the lower bound rather than the upper bound.

Figures 4 and 5 show MPT bounds for our equilibrium impenetrable-sphere model for $\alpha = \beta = 10$ and 50, respectively, as a function of the volume fraction up to $\phi_2 = 0.60$. These bounds are again contrasted with the second-order HS bounds. Again one observes the same kind of qualitative features as described in the previous paragraph.

In Fig. 6 we present the second- and third-order bounds for a macroscopically homogeneous composite which consists of glass spheres embedded in an epoxy matrix. The preparation of this composite is described in detail by Smith.[7] For the fully cured samples about 200 days after preparation, the ratios were found to be $\beta = 28.5$, $\gamma_1 = 0.228$, and $\gamma_2 = 0.660$. The computed values of reduced effective shear moduli at various volume fractions up to 0.5 are shown as solid circles in Fig. 6. As one can easily see, the data lie between the third-order bounds, and up to a volume fraction of 0.4, the third-order lower bound is quite a good estimate of the data. At $\phi_2 = 0.5$, the experimental value is still closer to the lower bound than the upper one, but

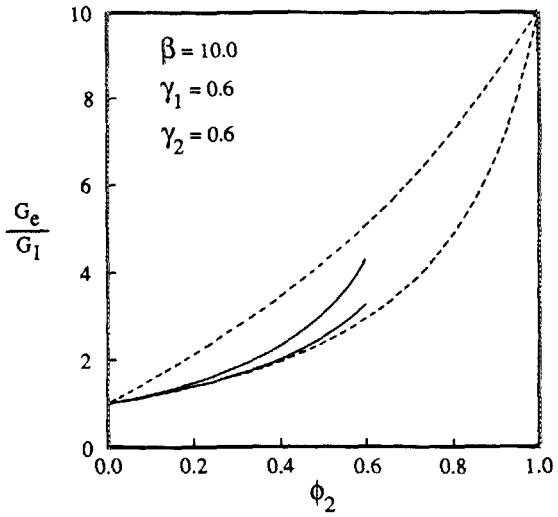

FIG. 4. Upper and lower bounds on the reduced effective shear modulus G_e/G_1 as a function of the sphere-volume fraction at $\alpha = K_2/K_1 = 10$ and $\beta = G_2/G_1 = 10$. Second-order HS bounds (dashed lines); third-order MPT bounds for the equal-sized random impenetrable-sphere model (solid lines). Here $\gamma_1 = \gamma_2 = 0.6$.

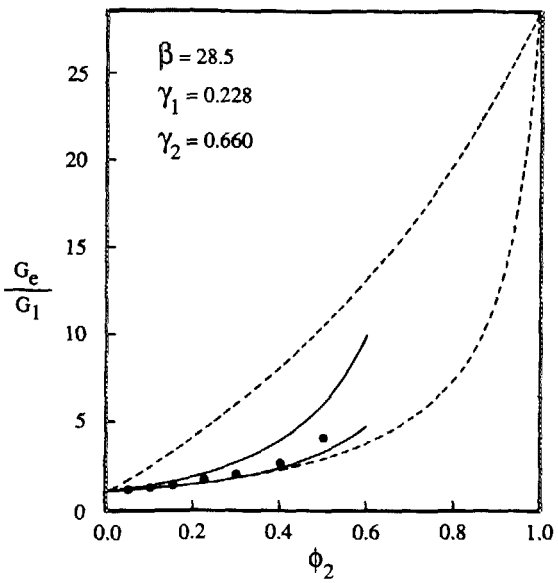

FIG. 6. Upper and lower bounds on the reduced effective shear modulus G_e/G_1 as a function of ϕ_2 at $\beta = 28.5$, $\gamma_1 = 0.228$, $\gamma_2 = 0.660$. HS bounds (dashed lines); MPT bounds (solid lines); and filled circles are Smith's data (Ref. 7) on effective shear modulus for spherical glass beads in an epoxy matrix.

not as close to the lower bound as at lower volume fractions. It is not clear whether this is due to scatter in the data or to particle contacts which may be present in the glass-epoxy system at such large ϕ_2. However, for the model we are considering the average coordination number (i.e., the average number of spheres physically touching each other) is identically zero for all ϕ_2 except at the maximum value corresponding to the random close-packing volume fraction. Thus, if the deviation is not due to scatter in the data, it may be explained by the presence of physical contact between particles which has the effect of increasing both the parameters ζ_2 and η_2 compared to our theoretical model system.

Finally, in Fig. 7, we present the interesting case of rigid, impenetrable-spherical particles ($\beta = \infty$) in an incompressible matrix ($K_1 = \infty$, G_1 is finite, and thus $\gamma_1 = 0$). This limit is of interest because of the analogy with the fluid mechanical problem of determining the effective shear viscosity of a suspension of equal-sized rigid spheres in an incompressible fluid. Einstein[23] calculated the shear viscosity of such a system through first order in the volume fraction ϕ_2. Through linear order in ϕ_2, this problem is mathematically identical to calculating the reduced shear modulus G_e/G_1 for perfectly rigid spheres in an incompressible matrix. This analogy fails to hold for quadratic and higher-order terms in ϕ_2 since the distributions of the particles in the

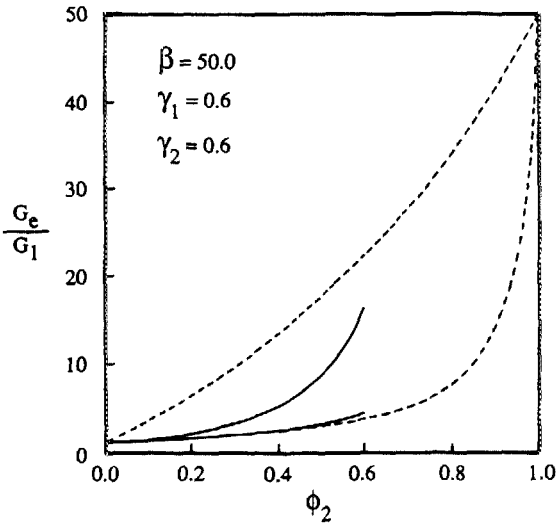

FIG. 5. As for Fig. 4 with $\alpha = \beta = 50$.

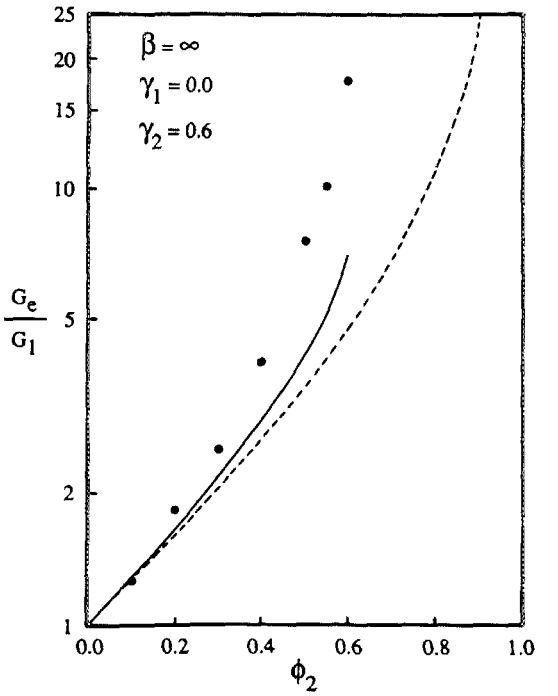

FIG. 7. Lower bounds on the reduced effective shear modulus G_e/G_1 as a function of ϕ_2 for rigid spheres ($\beta = \infty$) in an incompressible matrix ($\gamma_1 = 0$) and $\gamma_2 = 0.6$. HS lower bound (dashed line); MPT lower bound (solid line); and filled circles are Eilers' data (Ref. 8) on effective shear viscosity for bituminous particles in water. The upper bounds do not appear since they become infinite as $\beta \to \infty$.

two cases are different. In the case of a fluid suspension, the bulk motion will strongly affect the sphere configuration, whereas in the elasticity problem the infinitesimal applied strain has negligible effect on the sphere distribution. It may be mentioned here that for the case of effective shear modulus for the model under consideration, Chen and Acrivos[24] have obtained the coefficent of the ϕ_2^2 term exactly, and Torquato, Lado, and Smith[25] have evaluated the quadratic term for the third-order lower bound for partially penetrable spheres. In the results presented in Fig. 7, we give the second- and third-order lower bounds for this limiting case for any volume fraction (up to 0.6); the upper bounds do not appear because they tend to infinity in this limit. (The value $\phi_2 = 0.6$ corresponds to about 94% of the random close-packing value.[13]) Since no data were available for this limiting case of perfectly rigid spheres in an incompressible matrix, we have presented in Fig. 7 Eilers'[8] data (filled circles) on the relative shear viscosity for the suspension of bituminous particles in water, i.e., a case of rigid particles in an incompressible fluid. Such data points are expected to be somewhat higher than analogous shear modulus data.

V. CONCLUSIONS

The effective properties of random two-phase composites depend upon the microstructure of the composite through an infinite set of n-point probability functions. Apart from a few special cases, the infinite set of statistical functions is never known. Rigorous bounds, on the other hand, provide a means of estimating effective properties with limited but nontrivial microstructural information. In this paper, we computed bounds on the effective shear modulus of suspensions of random impenetrable spheres which require not only volume fraction information but the three-point parameters ζ_2 and η_2. The parameter η_2 was calculated here for this model for the first time. The third-order bounds are found to be restrictive enough to yield good estimates of the bulk properties up to about the random close-packing volume fraction even when the spheres are about two orders of magnitude more rigid than the matrix. Moreover, it is observed by comparison with the experimental data of Smith on the effective shear modulus of a glass-epoxy composite that the third-order lower bound lies very close to the data and serves as a very good estimate of the effective shear modulus for a volume fraction of up to about 0.45. Also, comparison of shear viscosity data of Eilers for bituminous particles in water indicates that even when the spheres are highly rigid relative to the matrix, the third-order lower bound itself serves as a reasonably good estimate of the bulk property for an appreciable range of ϕ_2. This latter fact is consistent with the general observation[20] that for $\beta \gg 1$, it is the lower bound rather than the upper bound which serves as a good estimate of the effective property, provided that the mean cluster size of phase 2 is much smaller than the scaled characteristic macroscopic length.

ACKNOWLEDGMENTS

A.K.S. and S.T. gratefully acknowledge support of the Office of Basic Energy Sciences, U. S. Department of Energy, under Grant No. DEFG05-86ER13482. F. L. wishes to acknowledge the support of the National Science Foundation under Grant No. CHE-84-02144.

[1] A. K. Sen, F. Lado, and S. Torquato, J. Appl. Phys. **62**, 3503 (1987).
[2] S. Torquato and F. Lado, Phys. Rev. B **33**, 6428 (1986).
[3] J. J. McCoy, *Recent Advances in Engineering Sciences* (Gordon and Breach, New York, 1970), Vol. 5, pp. 235–254.
[4] G. W. Milton and N. Phan-Thien, Proc. R. Soc. Lond. A **380**, 305 (1982).
[5] Z. Hashin and S. Shtrikman, J. Mech. Phys. Solids **11**, 127 (1963).
[6] L. J. Walpole, J. Mech. Phys. Solids **14**, 151 (1966).
[7] J. C. Smith, J. Res. NBS **80A**, 45 (1976).
[8] H. Eilers, Kolloid Z. **97**, 313 (1941).
[9] G. W. Milton, Phys. Rev. Lett. **46**, 542 (1981).
[10] Note that the definition of S_3 in Refs. 1 and 2 are different. S_3 in Ref. 2 refers to the three-point function for the matrix phase, but S_3 in Ref. 1 and in the present work refers to the three-point function for the particulate phase. This change makes the quantity K in Eq. (8) of Ref. 2 equal to the quantity $I[\hat{S}_3]$ used in the present work.
[11] J. P. Hansen and I. R. McDonald, *Theory of Simple Liquids* (Academic, New York, 1976).
[12] L. Verlet and J. J. Weis, Phys. Rev. A **5**, 939 (1972).
[13] J. G. Berryman, Phys. Rev. A **27**, 1053 (1983).
[14] J. D. Beasley and S. Torquato, J. Appl. Phys. **60**, 3576 (1986).
[15] G. W. Milton, in *Physics and Chemistry of Porous Media*, edited by D. L. Johnson and P. N. Sen (American Institute of Physics, New York, 1984).
[16] D. A. G. Bruggeman, Ann. Phys. (Leipzig) **24**, 636 (1935); See also R. Landauer, J. Appl. Phys. **23**, 779 (1952); R. Hill, J. Mech. Phys. Solids **13**, 213 (1965); and B. Budiansky, *ibid.* **13**, 223 (1965).
[17] S. Torquato, G. Stell, and J. Beasley, Lett. Appl. Eng. Sci. **23**, 385 (1985).
[18] M. N. Miller, J. Math. Phys. **10**, 1988 (1969).
[19] S. Torquato and F. Lado (unpublished).
[20] S. Torquato, J. Appl. Phys. **58**, 3790 (1985).
[21] A. Coniglio, V. DeAngelis, and A. Forlani, J. Phys. A **10**, 1123 (1977).
[22] The scaled characteristic length of the sample is defined as the dimensional characteristic length of the sample divided by the length scale of microscopic inhomogeneity (in this case, the diameter of a spherical inclusion).
[23] A. Einstein, Ann. Phys. **19**, 289 (1906). English translation in *Investigations on the Theory of Brownian Motion* (Dover, New York, 1956).
[24] H. S. Chen and A. Acrivos, Int. J. Solids Struct. **14**, 349 (1978).
[25] S. Torquato, F. Lado, and P. A. Smith, J. Chem. Phys. **86**, 6388 (1987).